

Probing neural circuits in the zebrafish: a suite of optical techniques

Donald M. O'Malley,^{a,*} Qiang Zhou,^b and Ethan Gahtan^a

^a *Department of Biology, Northeastern University, 414 Mugar Hall, Boston, MA 02115, USA*

^b *Department of Neurobiology and Behavior, SUNY—Stony Brook, Stony Brook, NY, USA*

Accepted 31 December 2002

Abstract

The ability to image neural activity in populations of neurons inside an intact animal, while obtaining single-cell or subcellular spatial resolution, has led to several advances in our understanding of vertebrate locomotor control. This result, first reported in a 1995 study of motoneurons in larval zebrafish, was the beginning of a series of technical developments that exploited the transparency and simplicity of the larval CNS. Presented here, in chronological fashion, is a suite of imaging techniques that have extended the ability to probe and optically dissect neural control systems. Included are methodological details pertaining to: (1) the *in vivo* optical recording of neural activity, (2) the optical dissection of complex neural architectures, and (3) additional fluorescence imaging-based techniques for the anatomical and physiological characterization of these systems. These approaches have provided insights into the descending neural control of escape and other locomotive behaviors, such as swimming and prey capture. The methods employed are discussed in relation to complementary and alternative imaging techniques, including, for example, the Nipkow disk confocal. While these methodologies focus on descending motor control in the larval zebrafish, the extension of such approaches to other neural systems is viewed as a promising and necessary step if neurobiologists are to bridge the gap between synaptic and brain region levels of analysis. The efficiency of optical techniques for surveying the cellular elements of intricate neural systems is of particular relevance because a comprehensive description of such elements is deemed necessary for a precise understanding of vertebrate neural architectures.

© 2003 Elsevier Science (USA). All rights reserved.

Keywords: Zebrafish; Confocal; Calcium; Hindbrain; Brainstem; Locomotion; Spinal cord; Neuron; Ablation; Reticulospinal

1. Introduction

This report focuses on the optical investigation of the locomotor control systems of the larval zebrafish. A brief explanation of the recent intense interest in zebrafish biology is in order. The transparency of the embryonic and larval forms and the ease of mutating, breeding, and maintaining large numbers of animals have made the zebrafish widely popular for developmental genetic studies. Virtually every organ system and anatomical feature of the animal is under investigation, as highlighted by a special issue of the journal *Development* that describes thousands of mutant lines (Vol. 123, 1996). Particular attention has been paid to developmental processes within the CNS [1–4]. Zebrafish

larvae exhibit a complex behavioral repertoire [5,6], yet the animal is sufficiently “simple” that many neurons in the brain and spinal cord can be individually identified both in fixed tissue [7,8] and *in vivo* [9–11]. Larval zebrafish thus provide a unique opportunity to investigate cellular-level details of the complex neural architectures that control locomotive behaviors.

While the application of optical techniques to the study of identified neurons might seem limited to larval zebrafish, an alternative view is that this is a first step toward a more comprehensive analysis of the very complex neural systems found in higher vertebrates. Taking this step, however, entails dealing with two formidable obstacles: (1) the possibility that the extent of neuronal phenotypic diversity is extreme [12,13], and (2) the inherent limitations in attempting to explain the function of a neural system where many elements are unexplored or unknown. Optical methods appear to be well suited for dealing with such problems

* Corresponding author. Fax: 1-617-373-3724.

E-mail address: d.omalley@neu.edu (D.M. O'Malley).

and the larval zebrafish constitutes an attractive test case because the total number of neurons within discrete neural subsystems is limited. Thus the idea of performing comprehensive surveys and effective optical dissection of extended neural subsystems becomes feasible. A key realization arising from these experiments is that such a comprehensive approach is essential if one is to evaluate competing models of the neural architectures underlying motor control or other neural operations. This idea seems to have received scant attention outside invertebrate studies, but greater adoption of optical techniques may facilitate more comprehensive, cellular-level analyses of neural systems in other vertebrate animals.

2. General methods

2.1. Overview

Confocal microscopy is the common thread to the optical techniques described here. It allows precise measurement of optical signals anywhere in the brain or spinal cord of the larval zebrafish. *Laser scanning* confocal microscopy, in particular, is essential for key aspects of this project. This work relied on the use of the Bio-Rad MRC 600, one of the first commercially successful confocal imaging systems. Although newer-model confocals offer additional features, this system operates at the limits of resolution of light microscopy and achieves an effective combined spatial–temporal resolution that has not been surpassed by newer systems. Some key features of the MRC 600 (and most other laser scanning systems) are a continuously variable aperture, simultaneous two channel recording, and flexible acquisition parameters. The significance of these features for particular experiments is described where appropriate, but a central theme is that the intensity and duration of laser illumination are always minimized so as to avoid or limit photodamage. This generally involves a trade-off between optical sectioning performance and light exposure.

The specific techniques to be discussed include: (1) recording of neural activity *in vivo*, (2) optical dissection of neural circuits followed by subsequent behavioral analysis, (3) correlation of neural activity with simultaneously recorded behaviors, and (4) filling of identified neurons by direct somal injections. All of these techniques involve the retrograde labeling of neurons with fluorescent-dextran-based tracers, some of which are fluorescent calcium indicators (calcium green dextran, Oregon green-BAPTA488 dextran) and some of which are just simple retrograde tracers (Texas red dextran, Alexa488 dextran); all are of the 10,000 MW variety (Molecular Probes, Eugene, OR). In all cases, confocal imaging has been used to visualize the labeled neurons in

intact larval zebrafish between 5 and 8 days old (post-fertilization).

2.2. General zebrafish handling and imaging techniques

Procedures for the maintenance of zebrafish colonies and the experimental manipulation of larval zebrafish have been described in detail elsewhere [14–16]. A brief summary of the procedures used in our experiments is as follows:

- Before injections or other experimental manipulations, larvae are anesthetized by immersion in 0.02% 3-aminobenzoic acid ethyl ester (MS222 or tricaine, Sigma chemical Co.). Larvae rapidly recover after removal of the anesthetic.

- Injections of fluorescent dextrans are usually made into ventral cord about half of the distance from the anal pore to the caudal end of the spinal cord. Larvae are injected with fluorescent dextrans (50% w/v in distilled water) under a dissecting microscope using microelectrodes pulled on a Sutter horizontal puller and broken back to a diameter of about one-third to one-half the diameter of the spinal cord.

- Batches of 24 larvae, aged 2 to 4 days posthatching, are typically injected and placed in 10% Hanks solution [14] in individual wells in a 24-well tissue culture tray. Larvae are usually examined the next day for the presence of desired labeling patterns. While the retrograde labeling may develop more quickly, it has not been necessary to determine this for our experiments.

- For imaging, larvae are anesthetized in MS222, and placed in a well in a Petri dish made by drilling a 1-cm-diameter hole and covering it with a square No. 1.5 coverslip. On the day of the experiment, the well is coated with an approximately 1-mm-thick layer of agar. After it solidifies, a narrow channel is cut out of the agar coating. The anesthetized larva is positioned in this channel dorsal side down so that the brainstem is as flat against the coverslip as possible. The larva is then covered with just molten agar to secure it in place (warm agar is kept in a VWR heat block at 42 °C). The MS222 is then wicked off and the larva and agar are covered with 10% Hanks solution. Care should be taken to ensure that the agar remains moist, as larvae at this age respire principally by oxygen diffusing through their skin.

- In most experiments, the larvae are imaged on an inverted Zeiss microscope using long-working-distance (>2.0 mm) objectives, either Olympus, 0.9 NA 60×, or Zeiss, 0.8 NA 40×. Higher-NA, medium-working-distance (~250 μm) objectives are available, but they do not provide access throughout the 300-μm depth of the larval hindbrain and, when looking at labeled neurons at depth in the hindbrain, did not yield dramatically better images than the more convenient long-working-distance objectives.

3. Specific techniques and examples

3.1. Calcium imaging of identified neurons in the larval brainstem

The techniques for labeling zebrafish neurons *in vivo* with fluorescent calcium indicators and subsequently monitoring neural activity in response to different sensory stimuli were developed at SUNY–Stony Brook [9,15; also see 17], and have since been applied to a number of neurobiological problems [11,18,19]. The general approach for studying brainstem neural activity takes advantage of the fact that many of the descending neurons project into far caudal spinal cord [20] and so populations of them can be retrogradely labeled by making a bulk injection into far caudal spinal cord (Fig.

1A), which does little harm to the larva. We routinely use fluorescent calcium indicators linked to 10,000 MW dextrans because these dextrans: (1) reliably label large populations of descending neurons; (2) are retained in the labeled neurons for many days if not weeks; (3) provide sufficient details of soma shape, position, and size, along with dendritic details and axonal trajectory, to allow conclusive identification of neurons *in vivo*; and (4) permit stable, potentially long-term recording of calcium activity in the intact larvae [15]. To our knowledge, all vertebrate neurons have voltage-activated calcium channels and therefore exhibit significant increases in somatic free calcium when firing one or more action potentials, making calcium a useful reporter of neural activity. While such an approach has limitations (temporal resolution of action potentials being the

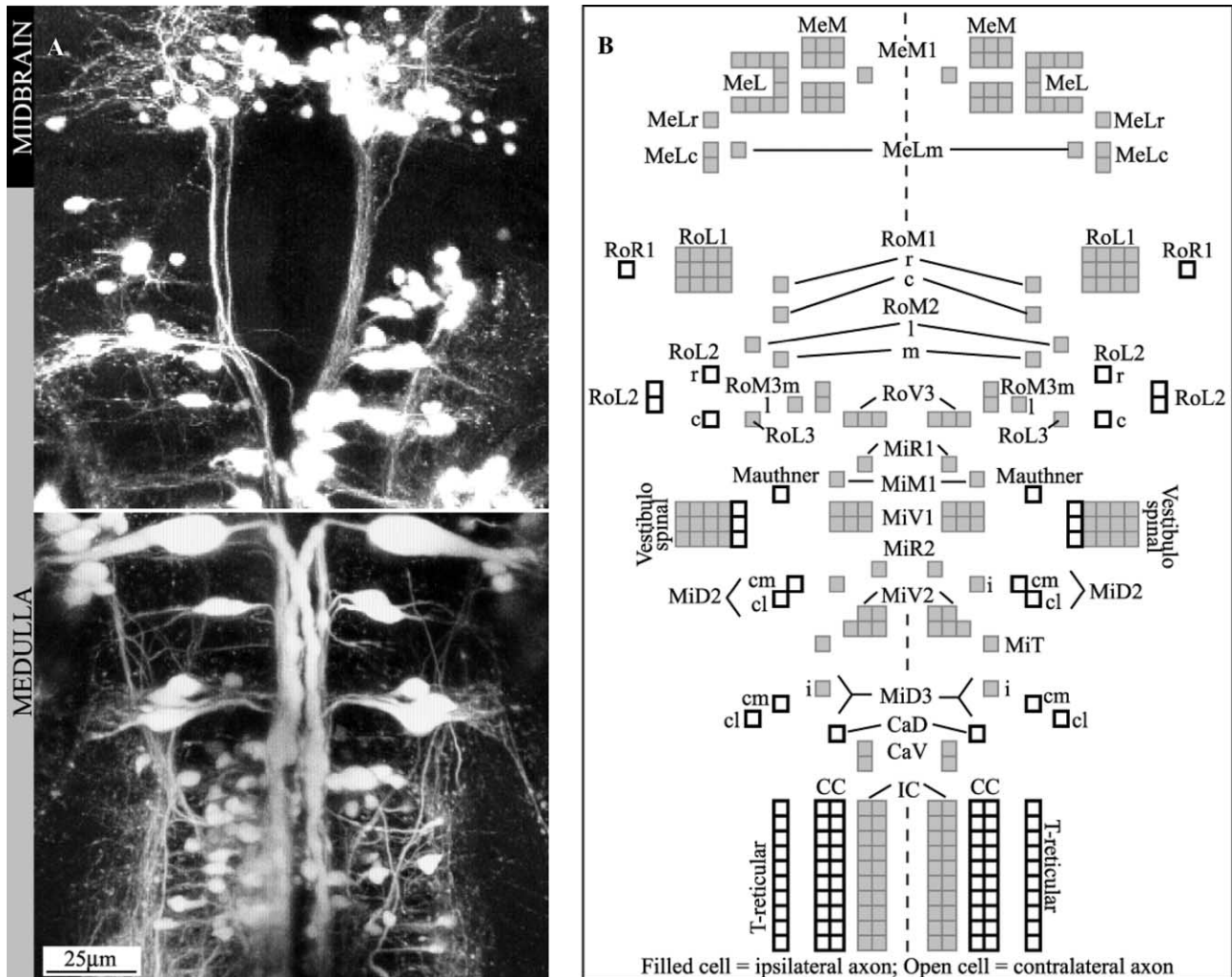


Fig. 1. Descending motor control system (DMCS) of the larval zebrafish. (A) Numerous neurons in the brainstem (medulla + midbrain) of a living 7-day-old zebrafish. Neurons were retrogradely labeled by injecting 10,000 MW fluorescent dextran into spinal cord (montage shows labeling from two different larvae). (B) Based on making many such injections, we have created a template designed to account for all descending neurons. Neurons are identified as either exact individuals (e.g., the Mauthner cells) or as members of small discrete clusters (e.g., RoL1 is a cluster of 12 neurons). Each box represents a single neuron, and the template can be used, for example, to record all neurons lesioned using either the laser ablation or labeled-lesion approach. The box representing each lesioned cell is checked and so the unchecked boxes represent the spared neurons. Behaviors that either are disrupted by the lesion or are instead maintained by the spared neurons are evaluated using a high-speed camera.

most serious), it has some advantages over competing methodologies and has yielded substantial new information about neurons that had been described anatomically 20 years ago, but for which there were no published physiological data.

The simplest type of imaging experiment is a “framescan,” where a series of small 2D images are acquired. Depending on the size and shape of the cell (or desired field of view), either 16 or 24 images are collected into the frame buffer at a rate a little faster than two images per second (Fig. 2). One might collect a greater number of smaller frames at a somewhat faster frame rate, but this is typically not useful in our experiments (a much faster imaging mode, called a *linescan*, is described below). The frame buffer is, in effect, one monitor screen of information (768×512 pixels) and so the 24-frame trial uses a 128×128 -pixel box size. The advantage of collecting just one frame buffer quantity of data per trial is that one does not have to write to disk during the trial, which would slow the acquisition rate significantly. The Bio-Rad MRC 600 offers a macro programming language for more complex acquisition protocols, an example of which is a time-lapse macro that we use to collect longer series of images at rates of 1 s/frame or slower (the write time from the frame-store to the hard disk is not an issue in such cases). Time lapse is useful for looking at more slowly occurring calcium signals, such as the effects of drug application on resting calcium levels. The framescan acquisition rate is best for routine surveying of neuronal responses to sensory stimuli: somal calcium signals rise quickly, but decay more slowly [21]. Framescans make it easy to determine if a neuron was active. The cell is zoomed in so that most of the

acquisition box is filled, but without cutting off the edges of the cell. This enhances the signal-to-noise ratio by maximizing the number of pixels of information per frame. We focus at the brightest focal plane just prior to each trial. Within the trial, several baseline images are collected prior to stimulation of the larva. Any increases in fluorescence that are time-locked to the stimulus are thus most likely due to activity-induced calcium fluxes. Because calcium transients have distinctive decay rates, further confirmation that these are bona fide calcium signals is provided by the decay time course, much of which is recorded during a typical framescan. Removal of extracellular calcium would provide the most direct confirmation of the nature of these in vivo fluorescence signals but that is not a viable option for this preparation. Other characteristics, however, such as the inward diffusion of calcium and the accumulation of calcium with trains of stimuli [9], as well as the enhancement of calcium signals by caffeine, mirror the calcium signals observed in cultured neurons and provide compelling evidence as to their nature.

In instances where better temporal resolution of the calcium responses is required, 2-ms linescans are used. In these one-dimensional images, a chosen line across the specimen (384 pixels long) is scanned at 2-ms intervals and these lines are displayed sequentially from top to bottom down the monitor (Fig. 3). This makes it possible to visualize either the diffusion of calcium in single neurons or the latency of calcium responses when simultaneously imaging multiple neurons [9,11,15,18, 21]. In this imaging mode it is sometimes possible to identify the individual line at which a calcium response began, yielding (at times) 2-ms resolution of the onset of

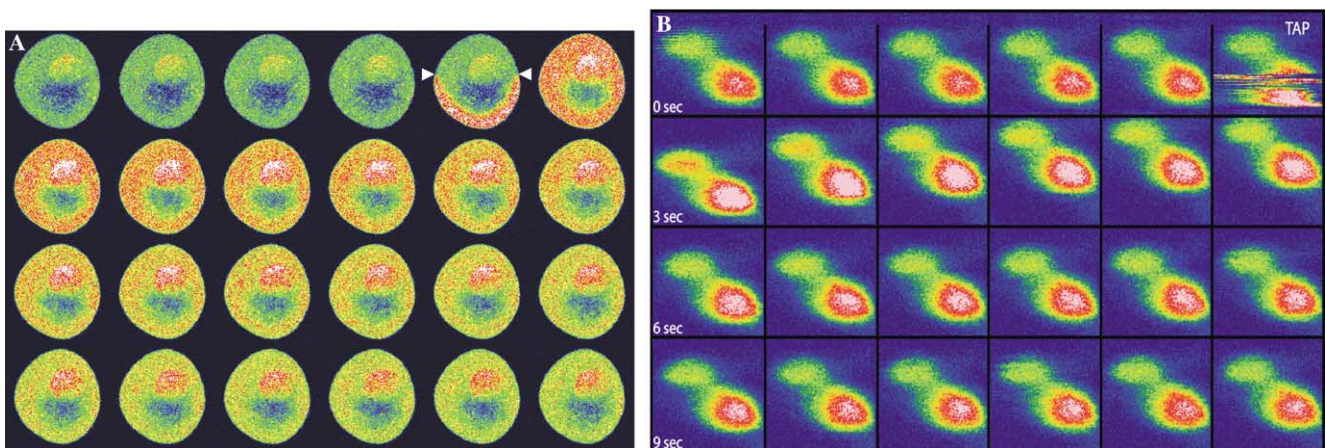


Fig. 2. Framescan recordings detect calcium responses and neural activity. (A) Early patch-clamp recordings of cultured bullfrog sympathetic neurons [21] established the normal relationship between electrical activity and calcium responses. Four baseline frames or images are shown, and midway during the fifth frame, the cell was depolarized for 50 ms to open voltage-gated calcium channels. (B) In a living zebrafish, the same protocol is used (frames are collected at 440-ms intervals), and the two cells shown (which are nearly coplanar here) both show fluorescence responses after a gentle tap to the head. The larva tries to escape, producing a sizable movement artifact in the last frame in the top row, but because it is embedded in agar the cells come back to the same position after the movement. Calcium rises quickly on stimulation, but decays slowly. Fluorescence increases evident after the movement reveal that both cells have fired one or more action potentials [9,15,18]. Subthreshold stimuli have never produced detectable somatic calcium responses in such experiments.

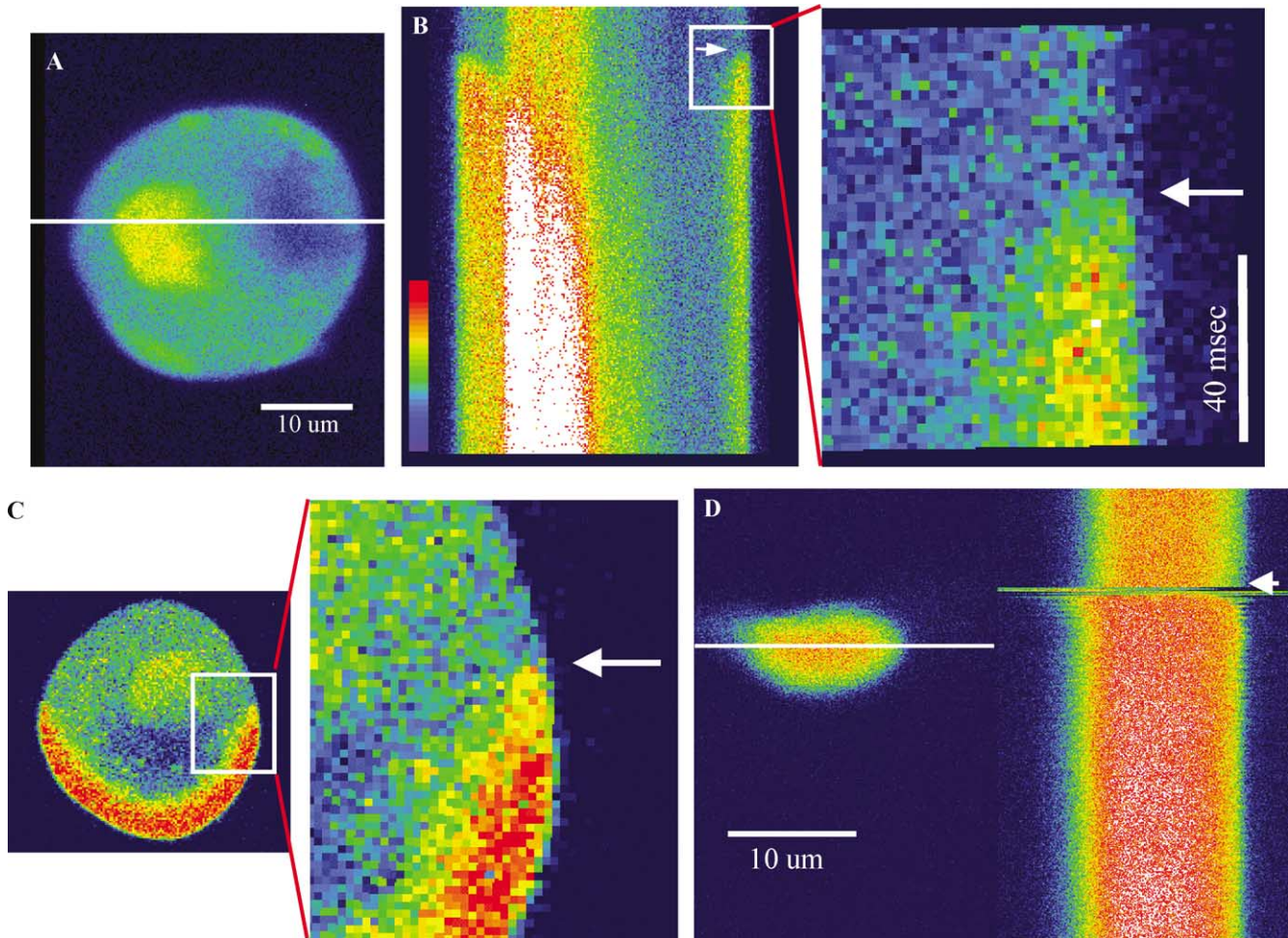


Fig. 3. Linescans provide spatial and temporal information about the dynamics of intracellular calcium signals. With laser-scanning confocal microscopes, a single line can be scanned repetitively at 2-ms intervals. The white line illustrated crossing the cell in (A) was scanned repeatedly (nucleus is yellow) and the scan lines are plotted from top to bottom in (B). The color scale indicates the relative fluorescence intensity, with blue being the lowest and red the highest; saturated pixels are colored white. At the time indicated by the arrow, the cell was depolarized for 50 ms. Calcium rushes in from both edges of the cell and, on the left side of the linescan, is observed diffusing toward and then across the nucleus. Magnification of the region in the white box reveals the spatial–temporal resolving power of laser-scanning confocal microscopy. The specific line (time) at which the fluorescence begins increasing (arrow) can be distinguished from the preceding lines. In addition, the diffusion of calcium into the cell can be resolved with submicron spatial resolution: each pixel is $0.2\ \mu\text{m}$ wide (and 2 ms high). Thus, this technique has a combined spatial temporal resolution of about $1\ \mu\text{m} \times 1\ \mu\text{m} \times 2\ \text{ms}$, or $2\ \mu\text{m}^2\text{-ms}$. (C) Individual framescans are also in effect “linescans,” although the line is being moved down the specimen with each successive scan. This is evident in a zoomed region of the right edge of the cell, where calcium is initially confined within a few pixels of the membrane, but some milliseconds later has diffused several micrometers into the cell. The persistent fluorescence gradient between nucleus and cytosol (evident after calcium has equilibrated across the cell in B) is due to the fact that fluorescent dyes behave differently in the nucleus and cytosol and so fluorescence (or ratiometric) signals must be independently calibrated in those regions [21,34]. (D) Because zebrafish CNS neurons are of small size and are deep in the brain, the diffusion of calcium is not so evident (head tap occurs at arrow). Linescans, however, do resolve the onset of the calcium response, within the limitations of the movement artifact, and can be used to scan multiple cells simultaneously, as was used to show co-activation of motoneurons [9] and brainstem neurons [18]. To obtain better latency determinations, larvae can be paralyzed with curare, which eliminates the escape-movement artifact [11].

a response. In addition, it is often possible to resolve the onset of calcium signals within $1\ \mu\text{m}^2$ (or less) of the plasma membrane. Thus, a laser scanning confocal microscope (LSCM) is potentially capable of obtaining a combined spatial–temporal resolution, albeit along a single line, of $2\ \mu\text{m}^2\text{-ms}$. This degree of spatial and temporal resolution is not always obtained; it may be less depending on the size of the signal or optical characteristics of the preparation. Still, to our knowledge, this is the best combined spatial–temporal resolution

that has been obtained in the dynamic imaging of neuronal activity. Voltage probes offer faster temporal resolution, but only by averaging or binning spatially over much larger areas. Because increases in temporal resolution better than 0.5 ms would add little in the way of useful information, we do not believe that current voltage dyes, when imaging activity within tissues or animals (cell culture is different matter), can usefully exceed the $2\ \mu\text{m}^2\text{-ms}$ combined spatial–temporal resolution of the laser scanning systems.

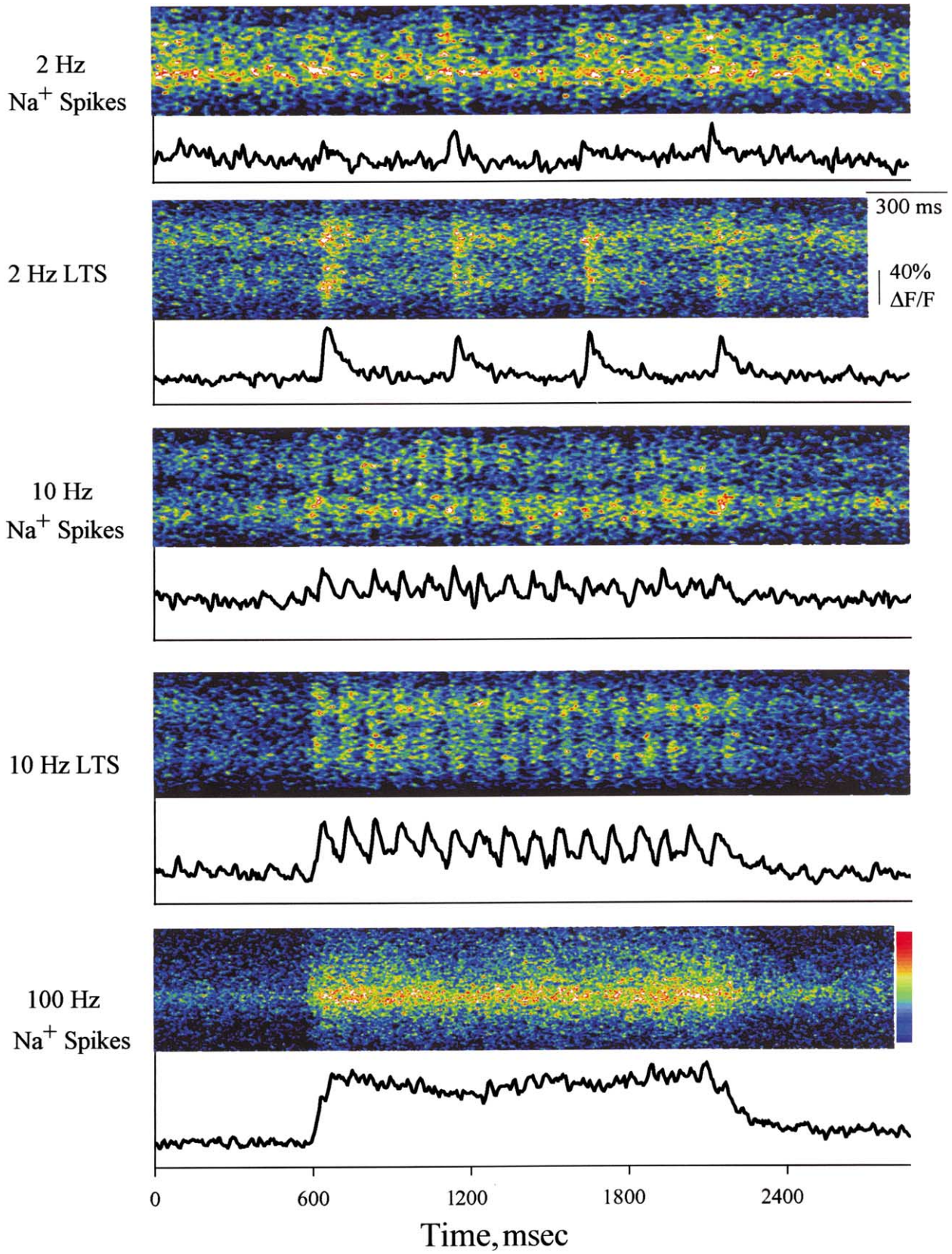
3.2. Options and trade-offs in confocal calcium imaging

The utility of linescanning confocal microscopes has been demonstrated in diverse applications, such as studies of calcium sparks [22], auditory hair cell functioning [23], and biophysical aspects of neuronal arbors and dendritic spines [24–26]. A newer type of confocal uses a Nipkow disk and provides considerably higher full-frame scan rates than laser scanning confocals [27–29]. Because these Nipkow disk confocals scan an entire field at once (using many points of light), they might, in theory, be expected to exceed the “ $2\mu\text{m}^2\text{-ms}$ ” combined resolution of linescans. While linescan imaging of calcium dynamics has been done for more than 10 years [30], commercial Nipkow disk instruments that use microlenses have only recently become available and their dynamic imaging potential is just beginning to be explored [31,32]. Examples of Nipkow disk instruments exceeding the performance of linescanning confocals in intact preparations have yet to be published, but a recent study mapping neural activity in pituitary slices, imaged at 5 Hz, has shown good signal-to-noise of calcium responses and sample stability (A. Hernandez-Cruz, unpublished observations). Use of an intensified CCD camera is currently being tested to determine if higher-temporal-resolution imaging can be obtained while maintaining slice viability. For both types of confocal, more intact preparations (slices, intact animals) tend to be more robust than cultured neurons. A significant drawback to Nipkow disk systems is that they do not have the variable pinhole aperture of LSCM instruments, which is often helpful in optimizing physiological experiments. For example, when studying neurons in the zebrafish brainstem, the pinhole aperture (on the MRC600) is often set at its full open position. This allows the illumination intensity to be sharply decreased, while still obtaining acceptable spatial resolution. The activity of single neurons has been recorded in experiments consisting of more than a hundred trials over a period of 2 days [15]. At the end of each physiological study, the laser power is increased and the confocal aperture closed to obtain a detailed anatomical reconstruction of the recorded neurons. Whether or not the aperture limitations of Nipkow disk confocals will preclude them from usefully exceeding the $2\mu\text{m}^2\text{-ms}$ resolution of linescans is one of the most significant questions to consider in future evaluations of these alternative technologies. Because Nipkow disks do not scan a single point, they are not well suited for laser ablation or fluorescence recovery after photobleach (FRAP) experiments.

The chief limitation when using calcium imaging to monitor neural activity is the slow decay of somatic calcium signals. Although dendritic calcium signals have faster kinetics, the ability of calcium imaging to resolve action potentials at high frequency is still limited. The

rate of calcium decay is determined mainly by the time required for calcium exchangers and pumps to remove calcium from the cytosol, although the off-rates of fluorescent calcium indicators (the time in which they release calcium when free calcium is falling) may contribute to this. In short, one cannot count action potentials unless they are well separated in time (Fig. 4, upper traces). Such limitations are offset by the variety of data that can be acquired. For example, linescanning of the Mauthner cell reveals that large calcium signals arise synchronously across the soma, axon hillock, and lateral dendrite [15,33]. In addition, by linescanning multiple neurons, the relative onset of neural activity can be determined [11,18]. It is also possible to detect individual action potentials, although the fluorescence responses are small; signals are usually binned over the entire soma or a length of dendrite. In addition, when action potentials occur in rapid succession (where they cannot be temporally resolved) the calcium responses will typically summate, causing a ramp increase in calcium levels (Fig. 4, lower trace). Measuring the size of the calcium responses associated with 1, 2, 5, and 10 action potentials [9,18] revealed that calcium indicators provide a rough estimate of the degree of neural activity, but not a perfect one, especially if calcium amplification mechanisms are occurring at the same time [33]. The calcium indicators we use are single-wavelength (i.e., nonratiometric) visible indicators. Ratiometric calcium indicators have some theoretical advantages over single-wavelength indicators (in terms of insensitivity to dye concentration and determination of resting calcium levels), but the superior dynamic range and lower phototoxicity of single-wavelength dyes, relative to currently available ratiometric indicators, have made them widely popular. These trade-offs are discussed in more detail in [34]. While calcium imaging has limitations, the ability to image the onset of neural activity and its relative magnitude and to image multiple neurons *in vivo* has provided a unique tool for the exploration of neural circuitry in the zebrafish.

This approach is particularly advantageous in zebrafish because so many neurons can be individually identified. For example, two brainstem neurons (MiD2cm and MiD3cm) were described in 1982 [7], proposed to be segmental homologues of the Mauthner cell in 1986 [20], and hypothesized to provide directional control of the escape behavior in 1993 [35], but it was not until the advent of the *in vivo* imaging technique that the first physiological recordings of these neurons were obtained [18]. This technique was originally viewed as a method for recording populations of individual neurons, and it is indeed possible to record from a dozen or more neurons simultaneously [9,36]. For most applications to date, however, calcium imaging has often proceeded from one cell to the next within individual animals [11,19], which is especially useful when neurons



can be individually identified [7,8,10; and see 37,38]. This allows the cellular elements of a system to be efficiently surveyed, yielding a comprehensive view of that system's functioning. This is more than a technical issue: knowing the number and types of neurons constituting a network is an essential step toward understanding the functioning of that network.

3.3. From correlation to causation: laser ablations and labeled lesions

Traditional lesioning approaches in vertebrate animals involve “regional” ablations, using, e.g., tract-cutting or electrolytic and neurotoxic lesioning methods. As such, these approaches affect substantial numbers of neurons which are unlikely to be identical in terms of connectivity and function. Instead, it is more likely that the afflicted population of neurons is highly heterogeneous and involved in multiple distinct and possibly conflicting behaviors, especially in brainstem where there is tremendous intermingling of cell types. But the brainstem is not unique, for a module of cerebral cortex has been suggested to contain between 300 and 3000 distinct cell types [13], while even a module of retina has been confirmed to have about 70 distinct cell types [12]. The heterogeneity in neuronal phenotype reported in these studies may be generally indicative of the organization of the CNS. If so, this would suggest that the complexity of the CNS is widely underestimated. Consequently, regional-level analyses may be reaching limits in terms of their utility for determining the precise functioning of vertebrate neural circuits. Cellular-level approaches that (1) attempt to obtain multimodal information on specific neurons and (2) are comprehensive in design, by seeking to examine all neurons involved in a specific computation or task, are deemed necessary for overcoming the limitations of regional approaches. The laser ablation of individually identified neurons is an example of a step in this direction.

Laser ablation of identified neurons has been useful in the investigation of invertebrate neural circuitry, as reviewed by Fetcho and Liu [39], and has recently been extended by these authors to the vertebrate CNS in a study of neurons involved in the C-start escape behavior. Focusing on the proposed segmental homologues of the Mauthner cell, MiD2cm and MiD3cm (collectively the “Mauthner array”), they found that laser ablation of

these three neurons eliminated the short latency of the escape response, while leaving the general pattern of the escape behavior intact [40]. These laser ablations are performed using the same laser-scanning confocals used in the calcium imaging experiments. The key difference is that during calcium imaging, the laser intensity is typically attenuated anywhere from 95 to 99%, greatly reducing light exposure. In addition cells are exposed only briefly and intermittently, i.e., only when acquiring images, helping to minimize photodamage. For laser ablations, the usual approach is to: (1) zoom in on the cell so that the scanning laser is focused on a small volume at the center of the identified cell; (2) increase the laser intensity to maximum (using a 15-mW argon–krypton laser); and (3) leave the laser beam “on” for an extended period, usually 10 min/cell. After laser ablation, larvae are released from the agar and allowed to recover overnight; behavioral assays of locomotor function are recorded the next day using high-speed digital imaging.

The laser ablation approach provides precise control over which cells live and which die and so has advantages over regional ablation techniques. It also has some advantages over the study of mutant strains of animals, as specific neural structures can be deliberately perturbed. Since brainstem neurons can be identified in larval zebrafish either individually or as members of small discrete clusters, this allows the optical dissection of any desired part of the descending motor control system (Fig. 5) after which one can evaluate (1) the impact of the lesion on the behavior of the animal and (2) whether or not the functioning of the remaining brainstem neurons has been affected. While the initial demonstration of this approach successfully produced a pronounced behavioral deficit, in terms of the latency of the escape behavior [40], much larger-scale laser ablations of the descending network failed to significantly disrupt other aspects of the larva's locomotive repertoire [41,42]. An obvious concern in interpreting this type of data is the reliability with which the lasing protocol is killing the targeted neurons.

3.4. Evaluation of the efficacy of laser ablations

During laser ablations, photobleaching is usually quite rapid and so the mere disappearance of a lased cell could reflect either cell death or photobleaching. In the study by Liu and Fetcho [40], several strategies were

Fig. 4. Resolution of low-frequency dendritic calcium responses using linescans. Neurons in rat thalamic slices were filled with calcium green and stimulated to fire either action potentials (Na^+ spikes) or low-threshold calcium spikes (LTS) at different frequencies; see [57] for more details. In both firing modes, calcium responses could be resolved at 2 and 10 Hz. At 100 Hz stimulation, calcium rapidly increases during the first 10 action potentials, and then remains elevated throughout the duration of the stimulus train, which ends at the end of the fluorescence plateau. Somewhat higher frequencies of response might be resolved, especially if a lower-affinity calcium indicator is used, such as *Fluo 4* dextran (not tested for this application yet). The plateau observed at 100 Hz does not appear to be due to saturation of the calcium indicator, but might instead reflect a complex interplay between the state of the voltage-gated calcium channels, the rate of calcium influx, and the capacity of calcium extrusion mechanisms, which is likely greater at higher calcium levels.

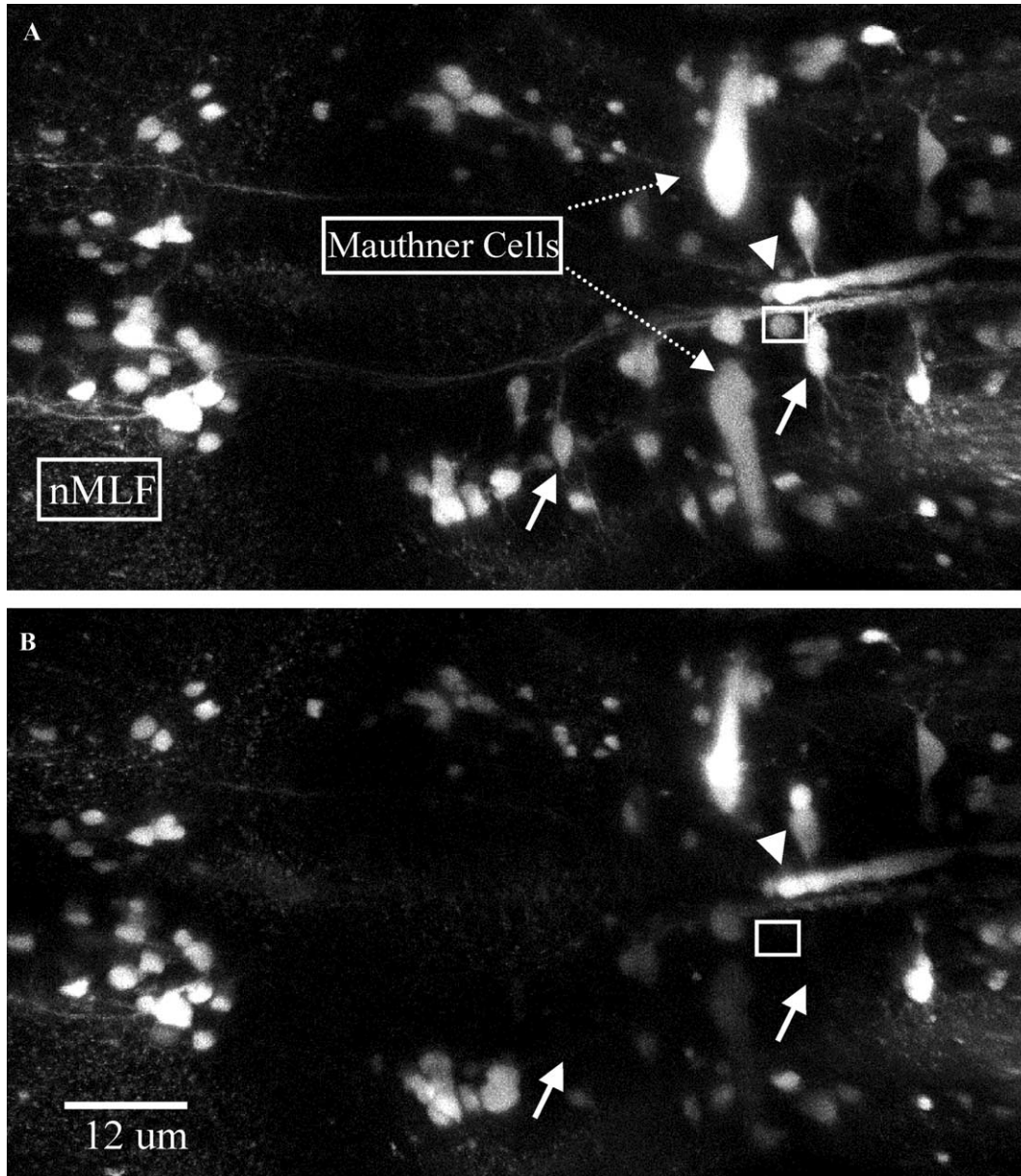


Fig. 5. Laser ablation of identified neurons in brainstem. (A) An array of medullary reticulospinal and mesencephalic nMLF neurons were labeled with Alexa488 dextran. Sustained lasing (7 min each) of the two neurons indicated by the solid arrows results in their complete and permanent disappearance. (B) No cells are evident in the regions where the two neurons were lased (arrows). Because of light scatter, cells in the vicinity of the lasing are now dimmer (e.g., cell in box in A), but they can generally be detected by increasing the laser power and typically have a normal appearance. This experiment demonstrates an unusual feature in that a Mauthner cell axon stump is evident (arrowhead), even though neither Mauthner cell was lased. The stump was formerly part of the lower Mauthner cell, which had a swollen, sickly appearance. In this particular example, these cells were labeled via an injection quite close to the juncture of brainstem and spinal cord. Cells labeled by this process normally survive, but close axotomy is known to be capable of causing cell death, and in this instance it appears that the lower Mauthner cell was undergoing such cell death. This is never observed when retrograde labeling injections are made at midtrunk or more caudally. Axon stumps are often observed after laser ablation [6], but not in every case.

employed to confirm cell killing. They observed axonal stumps (still fluorescent because the axonal dye is not bleached), together with an absence of the cell body, as viewed by DIC microscopy. This provided the most direct evidence of cell killing. A complementary double-labeling approach was also used. Descending neurons

were first retrogradely labeled with a mixture of red and green dextran (Texas red and calcium green dextran). Next the cell was killed using the red (568 nm) laser line: the red light damages the cell and photobleaches the red dye, but the second dye (visualized with the green 488-nm line) is intact. Nerve cells are not instantly destroyed

in these *confocal imaging laser*-based ablations, but instead exhibit a delayed cell death. Immediately after lasing, the green dye was still present, but by the next day the green dye and the cell had disappeared. Since this occurred without further lasing, this demonstrated that the cell was not simply photobleached, but had undergone a delayed loss of integrity, i.e., delayed cell death.

Several points should be noted regarding the attempted larger-scale ablations [41,42]. First, the cells being imaged are often smaller and “deeper” in the brainstem (when viewed from the dorsal aspect) than the Mauthner array, and so the cell-killing criteria of Liu and Fetcho [40] are not always applicable. Specifically, these deeper cells are not easily imaged via DIC. Also the ability to inflict lethal damage on double-labeled cells at one wavelength and retain sufficient unbleached dye at the second wavelength has not worked reliably, presumably because of the increased light scattering that occurs when focusing deeper into the brainstem which requires increased lasing time and results in more bleaching of both dyes. Axon stumps can often be observed (Fig. 5) and this provides more direct evidence that a cell has been disconnected from its spinal targets, if not killed outright. For unknown reasons, calcium indicators, such as calcium green dextran and Oregon green BAPTA488 dextran, appear to be more effective at killing cells than Alexa488 dextran, even though the latter dye appears brighter.

A third approach to confirm cell killing involves attempts to relabel neurons after laser ablation. Laser ablation experiments in which dozens of neurons were lased to a criterion (defined below) were followed by attempts to relabel the same neurons by making a second spinal injection, rostral to the first, with the goal of hitting undamaged axonal regions of some variable fraction of the lased population. In this experiment the initial labeling is done with a green dye, the cells are lased the next day, and a second injection is made (rostral to the first injection) using a red dye. While such injections retrogradely label large numbers of descending neurons, which neurons will be labeled cannot be precisely controlled. Nonetheless, the second injection often hits many of the same axons labeled by the first injection. Thus, one would predict that non-lased (still fluorescent) neurons can often be double-labeled while lased/killed cells can never be labeled with the second color tracer—because they no longer exist. This is exactly what was observed. While this is a statistical argument, it provides fairly strong evidence that most (if not all) of the lased cells have been killed: if large numbers of lased cells had survived, some of them should have been labeled with the second color dye. The fact that many nonlased cells can be double-labeled indicates that there was a sufficiently high probability of rehit axons of the lased cells. The

criteria adopted for deeming lased cells “dead” is that they show no somatic labeling when viewed the next day (16 to 24 h postlasing); i.e., there is no residual, circumscribed cell boundary, even when viewed with the strongest laser intensities. Residual punctate fluorescent debris is occasionally present in the vicinity of the missing cell, and this is viewed as further evidence of cell death. Based on these controls it appears that the “negative” results of the large-scale ablations reflect the biology of the descending control system, suggesting a highly distributed and/or redundant form of network organization.

The calcium imaging survey of escape-related activity [11] and complementary results [38], including studies of vestibular signal processing in lamprey [43,44], all suggest that widely distributed networks are used in descending motor control. These data are consistent with the resistance of such systems to disruption, but they complicate efforts to establish the cellular basis of these behaviors. More extreme measures are needed to effectively perturb such systems. One approach is simply to kill more neurons, but the confocal imaging laser takes an estimated 10 min to kill each individual cell. Based on a current estimate of 300 descending neurons in larval zebrafish, it is not feasible to eliminate a major fraction of the descending population. An attempt has been made to use a higher-powered nitrogen-pulsed laser to kill cells more quickly (E. Gahtan, unpublished observations) using, e.g., the MicroPoint system (Photonic Instruments, St. Charles, IL, USA), but there is often damage to blood vessels when attempting large-scale ablations, which would render lesion data uninterpretable. Two alternative/modified techniques have been developed for more extensive perturbation of the descending motor control system.

3.5. Large-scale lesioning of individually identified neurons

The first technique hinges on a study that investigated the method by which fluorescent dextrans retrogradely label neurons. The means by which 10,000 MW dextrans enter axons was previously uncertain. Two hypotheses were: (1) the injection pipet was severing the axons and the dextrans were entering through the open end of the axon before it resealed; (2) the injection was simply depositing dextran in the vicinity of the axons and the dextrans were crossing the plasma membrane and entering the cytosol, possibly due to some perturbation caused by the injection pipet. Recent evidence indicating that hypothesis 1 was correct [45] involved a double-label approach akin to the one described above. Twenty-four hours after injection of a red dye, a green dye is injected either rostral or caudal to the first injection. When the second injection is made *rostral* to the first injection some undamaged axons are hit as revealed by double labeling.

But when the second injection is made *caudal* to the first, double labeling of brainstem neurons is never observed, indicating that the axon was severed by the earlier injection at the more rostral site. Making such injections at the juncture between brainstem and spinal cord creates “labeled lesions” where descending neurons are not only labeled but are also simultaneously axotomized, thereby disconnecting them from their spinal targets. In instances where such injections labeled large numbers of neurons unilaterally in brainstem, the normal C-bend of the escape behavior was converted to an S-bend on just the side with the severed axons, confirming the efficacy of this approach [45]. While this approach does not allow one to precisely control which neurons will be axotomized, as a practical matter, many larvae can be rapidly injected (about two dozen per hour) and the resulting batch screened to find larvae with the desired labeled-lesion pattern. Because this technique can label and axotomize potentially very large numbers of neurons, it may be useful in other neural systems, especially in conjunction with two-photon imaging, which allows neurons to be visualized throughout the thickness of mammalian brain slice preparations [24–26].

To more quickly and specifically laser-ablate large numbers of neurons, without increasing collateral damage, a second large-scale lesioning method was developed [46]. Naga Sankrithi in our group has synthesized a phototoxic dextran by conjugating a photosensitizing agent, tin chlorin e6, to 10,000 MW dextran. This conjugate is injected in the same way as fluorescent dextrans. Preliminary experiments indicate that this decreases the required lasing time to <2 min per cell. At this rate, the killing of 100 to 200 neurons becomes feasible, at least to the extent that the larva's condition is not adversely affected by the sequential cell death (larvae tolerate embedding for up to 2 days at this age where the yolk sac is intact). In addition to allowing larger-scale, precisely targeted ablations, this approach allows a conceptually distinct *neuron-sparing experiment*, where the ablated neurons are “checked off” using a comprehensive template (Fig. 1B). This allows the spared (unchecked) neurons in the template to be correlated to any spared behaviors.

Neuronal sparing and neuronal ablation experiments are, in effect, two sides of the same coin. In each case, locomotive behaviors of the animal are evaluated using a high-speed camera to reveal both spared and impaired/eliminated behaviors. Both analyses are applicable to the labeled-lesion and chlorin-dextran techniques. These techniques are also complementary in that the chlorin-dextran experiments avoid mechanical damage in rostral spinal cord that occurs with labeled lesions, while the labeled-lesion experiments avoid damage that might result from the rupturing of large numbers of neurons in brainstem. If lesioning the same set of neurons produces the same behavioral deficit with both techniques, this

would eliminate the nonspecific damage peculiar to each technique as an explanation for the deficit.

3.6. Simultaneous imaging of *in vivo* neural activity and behavior

Correlation of neural activity with behavior is often done by recording electrically from neurons while animals are carrying out a behavior, often under some restraint that allows the experimenter to elicit and record the behavior of interest. A limiting factor in such experiments is that the exact identity of the recorded neuron may be uncertain, even if the tasks of sacrificing the animal and locating the recording site are carried out. Because of the potentially extreme diversity of neuronal phenotypes [12,13], it is quite difficult to be certain in successive experiments that one is recording from the exact same type of neuron. This is especially true in brainstem [47,48]. Even neurons with similar behavioral correlations and electrical response properties may have distinct inputs, outputs, and functions. Fortunately, in the larval zebrafish CNS, the exact same neurons can be examined from fish to fish and their input/output relationships and correlation to different behaviors determined more conclusively. To undertake behavioral correlation of neural activity in larval zebrafish, a relatively simple modification can be made, as first demonstrated by the Fetcho laboratory in a study of spinal interneurons [19]. As in the above calcium imaging experiments larvae are restrained in agar, but only the head is embedded. Escape-eliciting stimuli should now generate both calcium responses and tail movements, making it possible to correlate neural activity with “restrained behaviors” (Fig. 6).

To accomplish this, a high-speed CCD camera (Redlake Imaging, 500 frames per second) is attached to a Zeiss dissecting microscope (equipped with a trinocular tube) and mounted above an inverted confocal microscope. The dissecting scope is focused on the tail portion of the larvae, which is left free to move during the embedding process. Thus, while the confocal laser beam is scanning neurons in the brainstem, the high-speed camera is recording simultaneous tail movements. This required several modifications to the imaging procedures. First, the region of the coverslip beneath the tail of the larva is covered with white tape to provide higher visual contrast for the recording of tail movements. Second, the high-speed camera requires fairly strong illumination which might interfere with the confocal imaging, since stray light is not completely rejected by the confocal optics. To avoid an artifactual increase in the confocal background illumination, the confocal image is acquired using a green/FITC filter cube and the larva's tail is illuminated with light filtered by a red-wavelength, long-pass filter. Finally, to synchronize the confocal neural recording with the behavioral recording, an LED

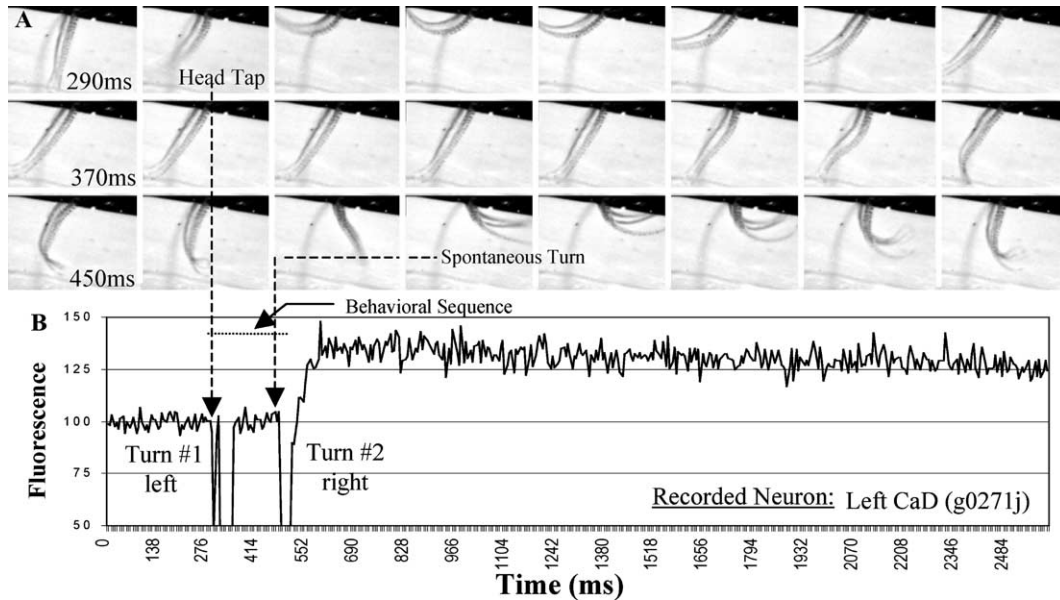


Fig. 6. Simultaneous imaging of neural activity and behavior. The larva's head is embedded in agar (occluded in dark region at top), while its tail is free to move. (A) A head tap given in the second frame causes a vigorous leftward tail movement which causes a downward deflection in the calcium imaging trace (B), but does not cause a detectable calcium increase (the transient decrease in fluorescence is caused by the cell moving out of the plane of focus, which precludes either ratiometric or single-wavelength measurement of calcium levels). In frame 3 in the third row, there is a vigorous, spontaneous rightward movement of the tail. This causes a brief deflection of the fluorescence trace, after which the fluorescence increases by more than 30%. The fluorescence then gradually decays throughout the remainder of the linescan. In this instance a slow linescan mode was used in which lines were scanned at 6-ms intervals.

was included in the optical path and its onset and offset times served as markers within the confocal recording. This approach is a minor variation of procedures originally described in a study of spinal interneurons [19].

An important *caution* should be noted: The optics of confocal microscopes are designed so that it is impossible for the viewer to look through the eyepieces and be exposed to a focused laser beam. Mounting an additional microscope above the stage of the inverted confocal microscope circumvents this normal safeguard so that it becomes a matter of operating procedures and user training to ensure that the confocal shutter is never opened while a user is peering through the dissecting scope. During the course of an experiment, this is usually not an issue: once the tail of the larvae has been focused on by the CCD camera, the camera is operated remotely by keyboard using the Redlake Imaging software. But when initially setting up the preparation, the larvae are viewed directly through the dissecting microscope and it is during this time that the confocal laser shutter must be kept closed.

While the tail movements of restrained larvae are not the same as the behaviors performed by free-swimming animals, they provide significant information about ongoing neuromuscular activity. Specific aspects of the tail movements, notably the laterality, amplitude, frequency, and latency, have direct implications for the activity of the underlying spinal neural circuitry. The spinal circuitry in turn is typically controlled or modu-

lated by descending signals. For example, examination of "restrained escapes" elicited by head taps revealed that in some instances the larva performs an isolated C-bend-like movement, while in other trials a complete escape-like behavior occurs (C-bend plus counterturn plus swimming-like tail movements). Being able to correlate neural activity in specific neurons to restrained locomotive behaviors provides clues to the organization of this system and immediately suggests laser-ablation experiments to test the necessity of those neurons for the behavior. To the extent that locomotive behaviors persist after comprehensively laser-ablating all neurons that were initially active during a behavior, this would suggest that a functional reorganization of the system had occurred. Such reorganization might be visualized by identifying neurons (from among the initially spared population) that are now active and have thus been recruited to support the spared behavior.

3.7. Extending the neuroanatomical database via fluorescence-guided techniques

In studies of the descending pathways of fish (e.g., goldfish, zebrafish) retrograde labeling techniques reliably reveal populations of descending neurons, providing sufficient details of the brainstem anatomy that neurons can often be individually identified [7,11,49–51]. Such studies failed, however, to reveal axonal branching patterns of these neurons in spinal cord. In mammals it

is well established that descending neurons, such as reticulo- and vestibulospinal neurons, have intricate, highly branched axon collaterals [48], but the extent to which such branching occurs in lower vertebrates was not known. The Mauthner cell has only short, stubby second-order branches [52,53], although these frequent branches do have powerful influences over spinal circuitry [54]. In an effort to determine the extent of spinal collaterals of other descending neurons, a double-labeling approach was used. First, a population of neurons is retrogradely labeled with Texas red dextran, labeling that is subsequently used to visually guide a microinjection pipet containing Alexa488 dextran to a specific identified neuron (Fig. 7A). In this approach the green channel is reserved for the single-cell injection because Alexa488 10K dextran is extremely bright and because there is little bleed through from the extensive red channel labeling into the green channel. Also, because the brainstem has to be injected through the dorsal aspect of the fish, the fish is embedded dorsal side up, versus dorsal side down which was used for the other

experiments described in this report. An upright microscope must therefore be used for this experiment.

Initially, confocal imaging was used to guide the microelectrode, but epifluorescence microscopy was found to be adequate when using long-working-distance 25× or 40× water immersion objectives. Sharp microelectrodes are difficult to use with intact larvae because of the toughness of their skin, so electrodes with tips in the size range of patch electrodes (3 to 5 μm) were used. The electrode is connected to a Picospritzer pressure injector (Parker Hannifin Corp., Fairfield, NJ, USA) and gentle suction is used to adhere the cell to the electrode tip. Puffs of air resulted in filling of the cell, which could be directly observed under fluorescence. Only one cell per larva was filled so that any labeled spinal collaterals could be unambiguously attributed to the targeted neuron. These experiments revealed that many of the descending neurons have extensive, highly branched axon collaterals [55]. In most cases, very thin primary collaterals were observed to branch perpendicularly off the stem axon at regular intervals along the

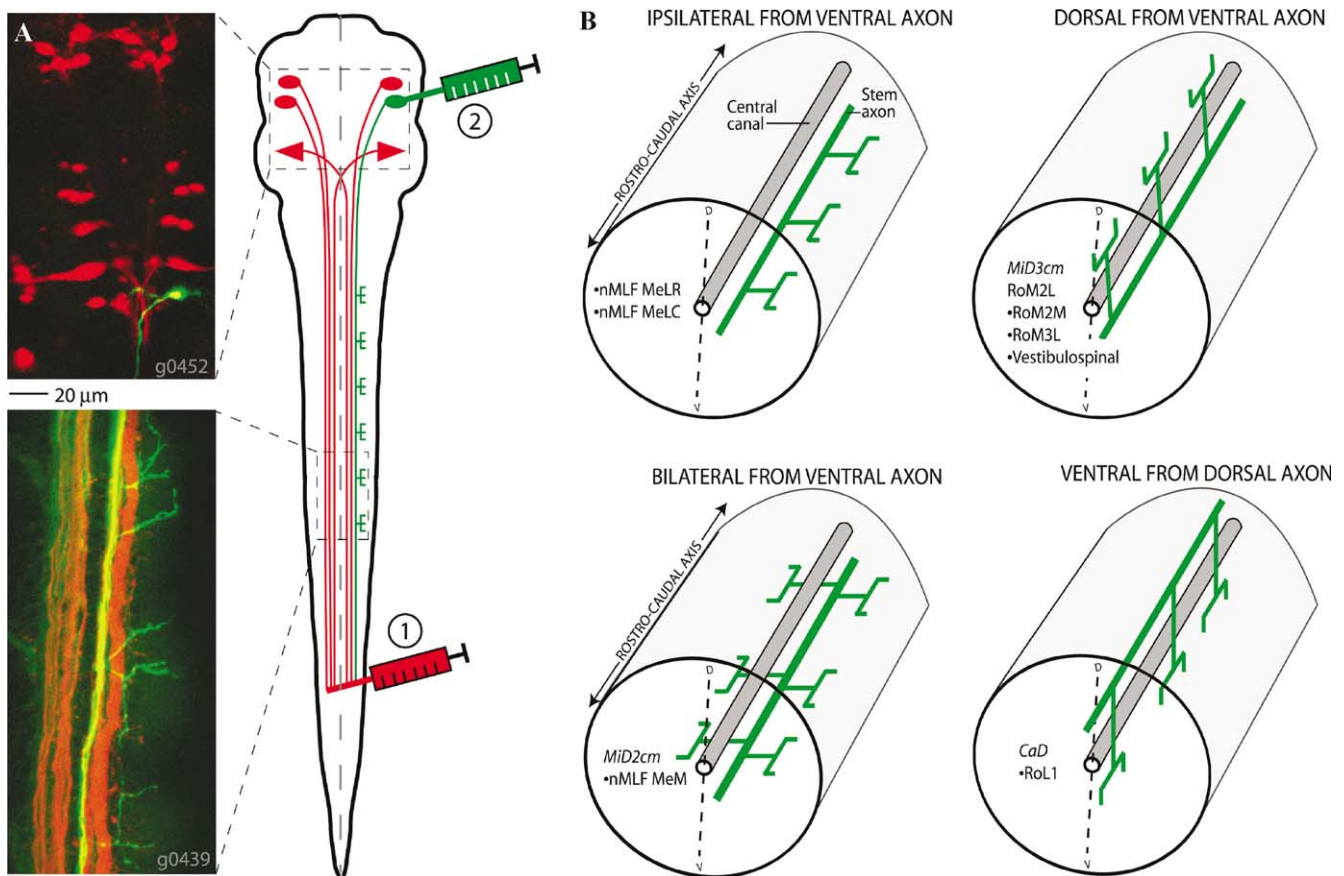


Fig. 7. Spinal axon collaterals of brainstem neurons visualized by direct injection of neuronal somata. (A) A population of neurons are first retrogradely labeled with Texas red dextran (top left panel). About 24 h later, a single specifically targeted neuron is injected with Alexa488 dextran (green). Direct injection of this bright tracer reveals axon collaterals in spinal cord (lower panel) that were not visualized by the Texas red labeling. Because of the small size of the larvae, these reticulospinal neurons can be reconstructed essentially in their entirety [55]; this has not been possible for descending neurons in other vertebrate animals. (B) A summary of the different cell types filled categorizes neurons based on the pattern of their axonal arbors. Each category is itself heterogeneous including cells with contralaterally projecting axons (italics) and cells with brainstem collaterals (bullets). This high degree of spinal arbor variability suggests a high degree of functional diversity among the 11 cell types thus far surveyed.

spinal cord. Overall, each type of descending neuron (of the 11 types initially surveyed) had its own distinctive and consistent spinal arborization pattern (Fig. 7B). These axonal arbors were not seen before because: (1) the amount of tracer entering via the very thin primary collaterals is quite small and difficult to visualize, and (2) retrograde fills generally label many descending neurons which obscures fine details that might otherwise have been visible. While these axon collaterals might be imaged directly on an upright confocal, the best results were obtained by quickly deembedding the larva (after brightly labeling a neuron), reembedding it dorsal side down flush against a coverslip, and then imaging it on an inverted confocal microscope.

The widespread rostral–caudal branching of axons exhibited by some descending neurons suggests that they directly influence every segment of the spinal cord. Other neurons, such as the nMLF cells, have collaterals restricted to rostral spinal cord. Also observed in this survey were several descending cell types that have axon collaterals in brainstem, suggesting that they may influence the processing of information in brainstem by local interneurons or descending neurons. Of particular interest would be the discovery of neurons that arborize only in far caudal spinal cord, as this might explain far caudal bends that are observed during prey capture swim bouts [6]. Only by comprehensively surveying all 40 known descending types can it be determined whether or not such cells exist.

4. Summary

The techniques described here individually offer insight into vertebrate neural architectures, but they are most powerful when used in combination. Having the anatomy, physiology, correlated behavior, and consequences of ablation of a specific neuron gives us a stronger basis for evaluating its role and, more importantly, for determining the type of neural architecture in which it is participating. While some features of the larval zebrafish CNS may not directly translate to other animals and experimental systems, to the extent that we can improve our ability to more conclusively (if not completely unambiguously) identify vertebrate neurons and study them repeatedly and via multiple techniques, this should advance our understanding of how vertebrate neural networks function. Of particular note is that optical techniques permit more comprehensive approaches than might be possible with nonoptical techniques. For example, being able to recognize many distinct cell types in an experimental preparation allows one to examine those cell types in a reasonably expeditious manner, as evidenced by the physiological and neuroanatomical surveys in zebrafish. While this is best done in “conventionally transparent” animals, such as

larval zebrafish, two-photon imaging greatly extends the depth to which cellular and synaptic details can be imaged in both brains slices [24] and living animals [25]. One cannot yet “comprehensively” study the entire hippocampus or cerebellum in a mammal, but an alternative is to comprehensively study neurons present in a reduced preparation, such as an acute or organotypic brain slice. If one only knows what 10% of the cells in a circuit are doing, does one have enough information to distinguish reorganizing from redundant from distributed [56] neural architectures? On the other hand, if one has detailed information about 90% of the cell types, one may feel more confident that one has seen enough of the system to understand how it works.

Acknowledgments

This work is supported by NIH Grants NS-37789 to D.M.O. and NS-11127 to E.G. We thank Barry Burbach and Seth Budick for technical assistance, Ms. Jeanette Campos for creating the initial version of the DMCS template, and Paul Adams for shaping the overall direction of this endeavor.

References

- [1] S.E. Brockerhoff, J.B. Hurley, U. Janssen-Bienhold, S.C.F. Neuhaus, W. Driever, J.E. Dowling, *Proc. Natl. Acad. Sci. USA* 92 (1995) 10545–10549.
- [2] J.L. Dynes, J. Ngai, *Neuron* 20 (1998) 1081–1091.
- [3] T. Nicolson, A. Rüschi, R.W. Friedrich, M. Granato, J.P. Ruppertsberg, C. Nüsslein-Volhard, *Neuron* 20 (1998) 271–283.
- [4] H. Baier, *Curr. Opin. Neurobiol.* 10 (2000) 451–455.
- [5] S.A. Budick, D.M. O'Malley, *J. Exp. Biol.* 203 (2000) 2565–2579.
- [6] M.A. Borla, B. Palecek, S.A. Budick, D.M. O'Malley, *Brain Behav. Evol.* 60 (2002) 207–229.
- [7] C.B. Kimmel, S.L. Powell, W.K. Metcalfe, *J. Comp. Neurol.* 205 (1982) 112–127.
- [8] R.R. Bernhardt, A.B. Chitnis, L. Lindamer, J.Y. Kuwada, *J. Comp. Neurol.* 302 (1990) 603–616.
- [9] J.R. Fetcho, D.M. O'Malley, *J. Neurophys.* 73 (1995) 399–406.
- [10] M.E. Hale, D.A. Ritter, J.R. Fetcho, *J. Comp. Neurol.* 437 (2001) 1–16.
- [11] E. Gahtan, N. Sankrithi, J.B. Campos, D.M. O'Malley, *J. Neurophys.* 87 (2002) 608–614.
- [12] M.A. MacNeil, R.H. Masland, *Neuron* 20 (1998) 971–982.
- [13] C.F. Stevens, *Curr. Biol.* 8 (1998) R708–R710.
- [14] M. Westerfield, *The Zebrafish Book: A Guide for the Laboratory Use of Zebrafish (*Brachydanio rerio*)*, Univ. of Oregon Press, Eugene, 1995.
- [15] J.R. Fetcho, K. Cox, D.M. O'Malley, *Histochem. J.* 30 (1998) 153–167.
- [16] D.M. O'Malley, J.R. Fetcho, in: R. Yuste, F. Lanni, A. Konnerth (Eds.), *Imaging Living Cells*, Cold Spring Harbor Laboratory Press, Cold Spring Harbor, NY, 2000, pp. 14.1–14.12.
- [17] M.J. O'Donovan, S. Ho, G. Sholomenko, W. Yee, *J. Neurosci. Methods* 46 (1993) 91–106.
- [18] D.M. O'Malley, Y.-H. Kao, J.R. Fetcho, *Neuron* 17 (1996) 1145–1155.

- [19] D.A. Ritter, D.H. Bhatt, J.R. Fetcho, *J. Neurosci.* 21 (2001) 8956–8965.
- [20] W.K. Metcalfe, B. Mendelson, C.B. Kimmel, *J. Comp. Neurol.* 251 (1986) 147–159.
- [21] D.M. O'Malley, *J. Neurosci.* 14 (1994) 5741–5758.
- [22] H. Cheng, W.J. Lederer, M.B. Cannell, *Science* 262 (1993) 740–744.
- [23] W. Denk, J.R. Holt, G.M. Shepherd, D.P. Corey, *Neuron* 15 (1995) 1311–1321.
- [24] K. Svoboda, D.W. Tank, W. Denk, *Science* 272 (1996) 716–719.
- [25] K. Svoboda, F. Helmchen, W. Denk, D.W. Tank, *Nat. Neurosci.* 2 (1999) 65–73.
- [26] R. Yuste, A. Majewska, S.S. Cash, W. Denk, *J. Neurosci.* 19 (1999) 1976–1987.
- [27] H. Tadakuma, J. Yamaguchi, Y. Ishihama, T. Funatsu, *Biochem. Biophys. Res. Commun.* 287 (2001) 323–327.
- [28] A. Egner, V. Andresen, S.W. Hell, *J. Microsc.* 206 (2002) 24–32.
- [29] T. Tanaami, S. Otsuki, N. Tomosada, Y. Kosugi, M. Shimizu, H. Ishida, *Appl. Opt.* 41 (2002) 4704–4708.
- [30] A. Hernandez-Cruz, F. Sala, P.R. Adams, *Science* 247 (1990) 858–862.
- [31] C. Genka, H. Ishida, K. Ichimori, Y. Hirota, T. Tanaami, H. Nakazawa, *Cell Calcium* 25 (1999) 199–208.
- [32] H. Ishida, C. Genka, Y. Hirota, H. Nakazawa, W.H. Barry, *Biophys. J.* 77 (1999) 2114–2122.
- [33] D.M. O'Malley, J.R. Fetcho, *Soc. Neurosci. Abstr.* 22 (1996) 795.
- [34] D.M. O'Malley, B.J. Burbach, P.R. Adams, in: S. Paddock (Ed.), *Confocal Microscopy: Methods and Protocols*, Humana Press, Totowa, NJ, 1999, pp. 261–303.
- [35] M.B. Foreman, R.C. Eaton, *J. Neurosci.* 13 (1993) 4101–4113.
- [36] J.R. Fetcho, D.M. O'Malley, *Curr. Opin. Neurobiol.* 7 (1997) 832–838.
- [37] R.C. Eaton, R.K.K. Lee, M.B. Foreman, *Prog. Neurobiol.* 63 (2001) 467–485.
- [38] T.J. Bosch, S. Maslam, B.L. Roberts, *J. Comp. Neurol.* 439 (2001) 306–314.
- [39] J.R. Fetcho, K.S. Liu, *Ann. NY Acad. Sci.* 860 (1999) 333–345.
- [40] K. Liu, J.R. Fetcho, *Neuron* 23 (1999) 325–335.
- [41] S. Budick, D.M. O'Malley, *Soc. Neurosci. Abstr.* 26 (2000) 158.
- [42] E. Gahtan, D.M. O'Malley, *Soc. Neurosci. Abstr.* 26 (2000) 158.
- [43] T.G. Deliagina, G.N. Orlovsky, S. Grillner, P. Wallen, *Exp. Brain Res.* 90 (1992) 489–498.
- [44] G.N. Orlovsky, T.G. Deliagina, P. Wallen, *Exp. Eye Res.* 90 (1992) 479–488.
- [45] E. Gahtan, D.M. O'Malley, *J. Neurosci. Methods* 108 (2001) 97–110.
- [46] N.S. Sankrithi, A. Purohit, G.B. Jones, D.M. O'Malley, *Soc. Neurosci. Abstr.* 28 (2002) 208.11.
- [47] J.M. Siegel, K.S. Tomaszewski, *J. Neurophys.* 50 (1983) 696–716.
- [48] S.I. Perlmutter, Y. Iwamoto, L.F. Barke, J.F. Baker, B.W. Peterson, *J. Neurophys.* 79 (1998) 285–303.
- [49] C.B. Kimmel, W.K. Metcalfe, E. Schabtach, *J. Comp. Neurol.* 233 (1985) 365–376.
- [50] R.K.K. Lee, R.C. Eaton, *J. Comp. Neurol.* 304 (1991) 34–52.
- [51] R.K.K. Lee, R.C. Eaton, S.J. Zottoli, *J. Comp. Neurol.* 329 (1993) 539–556.
- [52] M.R. Celio, E.G. Gray, G.M. Yasargil, *J. Neurocytol.* 8 (1979) 19–29.
- [53] G.M. Yasargil, C. Sandri, *J. Neurocytol.* 19 (1990) 111–126.
- [54] K.R. Svoboda, J.R. Fetcho, *J. Neurosci.* 16 (1996) 843–852.
- [55] E. Gahtan, D.M. O'Malley, *J. Comp. Neurol.* 459 (2003) 186–200.
- [56] D.W. Morton, H.J. Chiel, *Trends Neurosci.* 17 (1994) 413–420.
- [57] Q. Zhou, D.W. Godwin, D.M. O'Malley, P.R. Adams, *J. Neurophys.* 77 (1997) 2816–2825.